

External validation of unsupervised COVID-19 clinical phenotypes and their prognostic impact

Daniele Roberto Giacobbe, Emilio Di Maria, Alberto Stefano Tagliafico, Martina Bavastro, Carlo Simone Trombetta, Cristina Marelli, Gabriele Di Meco, Greta Cattardico, Sara Mora, Alessio Signori, Antonio Vena, Malgorzata Mikulska, Chiara Dentone, Bianca Bruzzone, Bianca Bignotti, Andrea Orsi, Chiara Robba, Lorenzo Ball, Iole Brunetti, Denise Battaglini, Antonio Di Biagio, Maria Pia Sormani, Paolo Pelosi, Mauro Giacomini, Giancarlo Icardi & Matteo Bassetti

To cite this article: Daniele Roberto Giacobbe, Emilio Di Maria, Alberto Stefano Tagliafico, Martina Bavastro, Carlo Simone Trombetta, Cristina Marelli, Gabriele Di Meco, Greta Cattardico, Sara Mora, Alessio Signori, Antonio Vena, Malgorzata Mikulska, Chiara Dentone, Bianca Bruzzone, Bianca Bignotti, Andrea Orsi, Chiara Robba, Lorenzo Ball, Iole Brunetti, Denise Battaglini, Antonio Di Biagio, Maria Pia Sormani, Paolo Pelosi, Mauro Giacomini, Giancarlo Icardi & Matteo Bassetti (2023) External validation of unsupervised COVID-19 clinical phenotypes and their prognostic impact, *Annals of Medicine*, 55:1, 2195204, DOI: [10.1080/07853890.2023.2195204](https://doi.org/10.1080/07853890.2023.2195204)

To link to this article: <https://doi.org/10.1080/07853890.2023.2195204>



© 2023 The Author(s). Published by Informa UK Limited, trading as Taylor & Francis Group



[View supplementary material](#)



Published online: 13 Apr 2023.



[Submit your article to this journal](#)









[View related articles](#)



[View Crossmark data](#)

External validation of unsupervised COVID-19 clinical phenotypes and their prognostic impact

Daniele Roberto Giacobbe^{a,b} , Emilio Di Maria^{a,c} , Alberto Stefano Tagliafico^{a,d}, Martina Bavastro^{a,b}, Carlo Simone Trombetta^{a,e}, Cristina Marelli^b, Gabriele Di Meo^b, Greta Cattardico^{a,b}, Sara Mora^f, Alessio Signori^g, Antonio Vena^{a,b}, Malgorzata Mikulska^{a,b}, Chiara Dentone^b, Bianca Bruzzone^e , Bianca Bignotti^{d,h}, Andrea Orsi^{a,e}, Chiara Robba^{i,j} , Lorenzo Balli^{i,j}, Iole Brunetti^j, Denise Battaglini^j, Antonio Di Biagio^{a,b} , Maria Pia Sormani^g, Paolo Pelosi^{i,j} , Mauro Giacomini^f, Giancarlo Icardi^{a,e} and Matteo Bassetti^{a,b}

^aDepartment of Health Sciences (DISSAL), University of Genoa, Genoa, Italy; ^bClinica Malattie Infettive, IRCCS Ospedale Policlinico San Martino, Genoa, Italy; ^cUniversity Unit of Medical Genetics, Galliera Hospital, Genoa, Italy; ^dDepartment of Radiology, IRCCS Ospedale Policlinico San Martino, Genoa, Italy; ^eHygiene Unit, IRCCS Ospedale Policlinico San Martino, Genoa, Italy; ^fDepartment of Informatics, Bioengineering, Robotics and System Engineering (DIBRIS), University of Genoa, Genoa, Italy; ^gSection of Biostatistics, Department of Health Sciences (DISSAL), University of Genoa, Genoa, Italy; ^hDepartment of Experimental Medicine (DIMES), University of Genoa, Genoa, Italy; ⁱDepartment of Surgical Sciences and Integrated Diagnostics (DISC), University of Genoa, Genoa, Italy; ^jAnesthesia and Intensive Care, IRCCS Ospedale Policlinico San Martino, Genoa, Italy

ABSTRACT

Background: Hospitalized patients with coronavirus disease 2019 (COVID-19) can be classified into different clinical phenotypes based on their demographic, clinical, radiology, and laboratory features. We aimed to validate in an external cohort of hospitalized COVID-19 patients the prognostic value of a previously described phenotyping system (FEN-COVID-19) and to assess the reproducibility of phenotypes development as a secondary analysis.

Methods: Patients were classified in phenotypes A, B or C according to the severity of oxygenation impairment, inflammatory response, hemodynamic and laboratory tests according to the FEN-COVID-19 method.

Results: Overall, 992 patients were included in the study, and 181 (18%), 757 (76%) and 54 (6%) of them were assigned to the FEN-COVID-19 phenotypes A, B, and C, respectively. An association with mortality was observed for phenotype C vs. A (hazard ratio [HR] 3.10, 95% confidence interval [CI] 1.81–5.30, $p < 0.001$) and for phenotype C vs. B (HR 2.20, 95% CI 1.50–3.23, $p < 0.001$). A non-statistically significant trend towards higher mortality was also observed for phenotype B vs. A (HR 1.41; 95% CI 0.92–2.15, $p = 0.115$). By means of cluster analysis, three different phenotypes were also identified in our cohort, with an overall similar gradient in terms of prognostic impact to that observed when patients were assigned to FEN-COVID-19 phenotypes.

Conclusions: The prognostic impact of FEN-COVID-19 phenotypes was confirmed in our external cohort, although with less difference in mortality between phenotypes A and B than in the original study.

KEY MESSAGES

- Hospitalized patients with COVID-19 can be classified into different clinical phenotypes based on their demographic, clinical, radiology, and laboratory features
- In this study, we externally confirmed the prognostic impact of clinical phenotypes previously identified by Gutierrez-Gutierrez and colleagues in a Spanish cohort of hospitalized patients with COVID-19, and the usefulness of their simplified probabilistic model for phenotypes assignment
- This could indirectly support the validity of both phenotype's development and their extrapolation to other hospitals and countries for management decisions during other possible future viral pandemics


ARTICLE HISTORY

Received 2 January 2023
Revised 24 February 2023
Accepted 20 March 2023

KEYWORDS

COVID-19; SARS-CoV-2; phenotypes; pandemic; unsupervised clustering; external validation; prognosis

CONTACT Daniele Roberto Giacobbe  danieleroberto.giacobbe@unige.it  Department of Health Sciences (DISSAL), University of Genoa, Via A. Pastore 1 – 16132 Genoa, Italy

 Supplemental data for this article can be accessed online at <https://doi.org/10.1080/07853890.2023.2195204>.

© 2023 The Author(s). Published by Informa UK Limited, trading as Taylor & Francis Group.

This is an Open Access article distributed under the terms of the Creative Commons Attribution-NonCommercial License (<http://creativecommons.org/licenses/by-nc/4.0/>), which permits unrestricted non-commercial use, distribution, and reproduction in any medium, provided the original work is properly cited. The terms on which this article has been published allow the posting of the Accepted Manuscript in a repository by the author(s) or with their consent.

Background

Hospitalized patients with coronavirus disease 2019 (COVID-19) can be classified into different clinical phenotypes based on their demographic, clinical, radiology, and laboratory features [1–7]. Based on data from the first phase of the COVID-19 pandemic, Gutierrez-Gutierrez and colleagues identified three distinct clinical phenotypes through unsupervised clustering in a derivation cohort, and then assessed and validated their prognostic impact both in an internal validation cohort and in an external validation cohort from the same country (Spain) [4].

While the clinical picture and prognosis of COVID-19 in hospitalized patients have changed dramatically and favourably after 2020, especially with the availability of efficacious vaccines in preventing progression to severe disease [8,9], additional external validation from other countries of the prognostic impact of phenotypes remains crucial to confirm the reproducibility of both results and methodology. Indeed, this could prove useful during other possible future viral pandemics for guaranteeing rapid and solid extrapolation to different parts of the world of reliable research findings with relevant clinical implications.

In the present study, we aimed to validate the prognostic impact of clinical phenotypes developed by Gutierrez-Gutierrez and colleagues in an external cohort of COVID-19 patients hospitalized during the first phase of the pandemic in a large teaching hospital in Italy. In addition, we aimed to assess the reproducibility of phenotypes development in our cohort as a secondary analysis.

Methods

Setting and objectives

The present retrospective study was conducted at IRCCS Ospedale Policlinico San Martino, a 1200-bed teaching hospital in Genoa, Northern Italy. The study population was patients with COVID-19 hospitalized from January 2020 to April 2021. Exclusion criteria were: (i) age <18 years old; (ii) number of missing variables per patient <50%. The primary study objective was to validate the prognostic impact of the phenotypes developed by Gutierrez-Gutierrez and colleagues in our Italian cohort. Secondary objectives were: (i) to assess whether the unsupervised clustering of demographic and clinical variables from a subset of two third of patients from our study population (derivation cohort) resulted in clinical phenotypes similar to those obtained by Gutierrez-Gutierrez and colleagues; (ii) to

assess whether also the phenotypes identified in our derivation cohort exerted a prognostic impact in the derivation cohort and in the remaining one-third of patients (internal validation cohort).

The collection of anonymized data from hospitalized COVID-19 patients for research purposes was approved by the local ethics committee (Liguria Region Ethics Committee, protocol registry number 163/2020). A subsequent protocol amendment, reviewed by the same local ethics committee before the conduction of the present retrospective study, was approved in May 2021. Specific informed consent for this validation study was waived due to the retrospective nature of the analyses.

Definitions and data collected for the study

COVID-19 was defined as at least one positive real-time polymerase chain reaction test for SARS-CoV-2 on a respiratory specimen. Collected variables were defined as in the study by Gutierrez-Gutierrez and colleagues. In particular, we collected the following variables necessary for patients' assignment to the different phenotypes derived from the Spanish cohort: age; gender; body mass index; chronic lung disease; white blood cells count at admission; neutrophils count at admission; C-reactive protein at admission; diastolic blood pressure at admission; oxygen saturation without oxygen therapy at admission; serum creatinine at admission; serum potassium at admission; serum sodium at admission; hematocrit at admission; international normalized ratio at admission; blood glucose at admission. In addition, in order to assess the reproducibility of the development of phenotypes in our internal validation cohort, and to subsequently assess their prognostic impact, we were able to collect also the following variables employed by Gutierrez-Gutierrez for phenotypes development: chronic heart disease; hypertension; diabetes mellitus; chronic kidney disease; chronic liver disease; chronic neurologic disease; dementia; active solid malignancy; active hematological malignancy; human immunodeficiency virus/acquired immunodeficiency syndrome; treatment with angiotensin converting enzyme inhibitors; treatment with angiotensin receptor blockers; reported fever at admission; temperature at admission; myalgia/arthritis at admission; headache at admission; anosmia at admission; altered mental status at admission; lymphocyte count at admission; D-dimer at admission; procalcitonin at admission; interleukin-6 at admission; ferritin at admission; heart rate at admission; systolic blood pressure at admission; dyspnea at admission; cough at admission; expectoration at admission;

respiratory rate at admission; arterial PaCO₂; lung infiltrates on chest radiography at admission; serum albumin at admission; lactate dehydrogenase at admission; serum bilirubin at admission; hemoglobin at admission; platelet cells count at admission; creatine phosphokinase at admission.

Statistical analysis

The primary study analysis was the evaluation of the prognostic impact in our cohort of phenotypes developed by Gutierrez-Gutierrez and colleagues. We first performed multiple imputations by chained equations (MICE), employing the nearest neighbours-based predictive mean matching method (the proportion of missing data per variable in our cohort, compared with the Spanish cohort, is shown in [supplementary Table S1](#)) [10]. Then, we assigned each patient in our population to one of the three phenotypes (A, B, or C) previously identified by Gutierrez-Gutierrez and colleagues. This was done by using the FEN-COVID-19 website (<https://www.fen-covid.com>) for assigning each patient to the phenotype with the highest resulting probability of assignment. Subsequently, the cumulative incidence of 30-day mortality in patients assigned to the three different phenotypes was presented graphically with the Kaplan-Meier method, whereas the impact of the different phenotypes on 30-day mortality as a time-to-event endpoint was assessed by means of Cox regression after having verified fulfilment of the proportional hazard assumption through the log(-log(survival)) versus the log of survival time graph. Results were reported as hazard ratios (HRs) together with the corresponding 95% confidence intervals (CIs).

With regard to the study's secondary objectives, to reproduce the development of phenotypes in our cohort, we first randomly divided our population into a derivation cohort (composed of two third of patients) and an internal validation cohort (composed of one-third of patients). Subsequently, we assessed the distribution of variables in the derivation cohort. By means of the χ^2 test and Pearson's correlation coefficient for categorical and continuous variables, respectively, we excluded variables that were highly correlated, as reasonable proxies, to other variables ($\alpha < 0.01$), in order to avoid collinearity. Then, we performed a two-step cluster analysis using both categorical and continuous variables to obtain the optimal number of clusters based on the silhouette index. We did not perform a sensitivity analysis excluding variables with more than 50% missing data as in the study by Gutierrez-Gutierrez and colleagues, since all variables in our cohort had less than 50% missing data.

After the variables were grouped into different categories (comorbidities, system-related, or organ-related, as in the study by Gutierrez-Gutierrez and colleagues), we used chord diagrams and heatmaps to visualize the pattern of distribution of variables in the different phenotypes.

To verify the impact on mortality of phenotypes developed in our derivation cohort, we first developed a probabilistic model as done in the study by Gutierrez-Gutierrez and colleagues, in order to assign phenotypes and then verify their prognostic impact also in our internal validation cohort. To this aim, we performed a multinomial logistic regression analysis in the derivation cohort. We first compared variables between phenotypes using the χ^2 test and the Kruskal-Wallis test for categorical variables and continuous variables, respectively. Then, variables showing a potential association with phenotypes ($p < 0.20$) were included in a multinomial logistic regression model, excluding collinear variables based on the variance inflation factor, and selecting variables for the final model through a manual backward procedure. Convergence of the model was obtained by using Jeffreys-prior penalty of the likelihood [11]. The area under the receiver operating characteristic curve (AUROC) was employed to measure the predictive ability of the model for phenotype assignment. Finally, the impact of phenotypes on 30-day mortality was assessed as in the primary study analysis (see above), both in the derivation cohort and in the internal validation cohort.

The analyses were performed using R Statistical Software (version 4.2.1, R Foundation for Statistical Computing, Vienna, Austria), and SPSS Statistics for the two-step cluster analysis (Version 29.0. IBM Corp, Armonk, NY, US).

Results

Overall, 992 patients were included in the study. Their median age was 72 years (interquartile range [IQR] 50–82) and 62% were male (616/992). Their demographic and clinical characteristics are reported in [Table 1](#), which also shows the distribution of patients and variables in the three phenotypes previously developed by Gutierrez-Gutierrez and colleagues. Overall, 181 (18%), 757 (76%) and 54 (6%) patients were assigned to phenotypes A, B, and C, respectively. As shown in [Figure 1](#), the cumulative 30-day mortality was 60.9% in patients assigned to phenotype C, while it was 25.5% and 38.2% in patients assigned to phenotype A and phenotype B, respectively. An association with mortality in Cox regression models was observed

Table 1. Demographic and clinical characteristics of patients in the entire study population and after assignment to the phenotypes identified by Gutierrez-Gutierrez and colleagues*.

Variable	Study population			Phenotype A		Phenotype B		Phenotype C		P value
	No. of patients (%)	No. of patients (%)	No. of patients (%)	No. of patients (%)	No. of patients (%)	No. of patients (%)	No. of patients (%)	No. of patients (%)		
Demographics										
Age in years, median (IQR)	72 (59–82)	55 (43–67)	74 (63–83)	82.5 (73–89)						<0.001
Male sex	616 (62.1)	113 (62.4)	471 (62.2)	32 (59.3)						0.906
Comorbidities										
Chronic heart disease	82 (8.3)	5 (2.8)	65 (8.6)	12 (22.2)						<0.001
Hypertension	469 (47.3)	48 (26.5)	384 (50.7)	37 (68.5)						<0.001
Chronic lung disease	113 (11.4)	8 (4.4)	97 (12.8)	8 (14.8)						0.004
Chronic kidney disease	95 (9.6)	16 (8.8)	46 (6.1)	33 (61.1)						<0.001
Chronic liver disease	36 (3.6)	6 (3.3)	26 (3.4)	4 (7.4)						0.311
Chronic neurological disease	121 (12.2)	13 (7.2)	100 (13.2)	8 (14.8)						0.070
Active solid malignancy	63 (6.4)	7 (3.9)	49 (6.5)	7 (13)						0.053
Active hematological malignancy	32 (3.2)	11 (6.1)	19 (2.5)	2 (3.7)						0.050
HIV/AIDS	15 (1.5)	2 (1.1)	12 (1.6)	1 (1.9)						0.874
Obesity	40 (4)	6 (3.3)	31 (4.1)	3 (5.6)						0.751
Diabetes mellitus	154 (15.5)	15 (8.3)	122 (16.1)	17 (31.5)						<0.001
Dementia	93 (9.4)	4 (2.2)	81 (10.7)	8 (14.8)						<0.001
Treatments for underlying conditions										
Angiotensin converting enzyme inhibitors	113 (13.4)	13 (7.2)	114 (15.1)	6 (11.1)						0.016
Angiotensin receptor blockers	113 (13.4)	14 (7.7)	107 (14.1)	12 (22.2)						0.011
Infection data at diagnosis										
<i>Non-focal symptoms</i>										
Reported fever	790 (79.6)	139 (76.8)	615 (81.2)	36 (66.7)						0.021
Temperature in °C, median (IQR)	37.2 (36–38)	37.1 (36.1–38)	37.2 (36.2–38)	36.6 (36–37.6)						0.044
Myalgia/arthralgia	52 (5.2)	13 (7.2)	38 (5)	1 (1.9)						0.260
Headache	32 (3.2)	6 (3.3)	26 (3.4)	0 (0)						0.385
Anosmia	24 (2.4)	7 (3.9)	17 (2.2)	0 (0)						0.218
Altered mental status	90 (9)	8 (4.4)	75 (9.9)	7 (13)						0.058
<i>Inflammation</i>										
White blood cells × 10 ³ /mm ³ , median (IQR)	6.7 (4.8–9.2)	6.2 (4.3–8.3)	6.7 (4.9–9)	9.9 (6.1–15.8)						<0.001
Lymphocyte cells × 10 ³ /mm ³ , median (IQR)	0.9 (0.6–1.2)	1.1 (0.8–1.5)	0.8 (0.6–1.2)	0.6 (0.5–0.9)						<0.001
Neutrophil cells × 10 ³ /mm ³ , median (IQR)	5.1 (3.4–7.5)	4.3 (2.7–6.1)	5.1 (3.6–4)	7.9 (4.1–13.3)						<0.001
D-dimer in ng/mL, median (IQR)	1002.5 (595.9–1673.3)	748.3 (490.3–1246)	1018 (621.6–1673)	1517.5 (936.5–4158.3)						<0.001
Procalcitonin in ng/mL, median (IQR)	0.2 (0.1–0.43)	0.1 (0.0–0.3)	0.16 (0.1–0.4)	1.1 (0.5–4)						<0.001
C-reactive protein in mg/L, median (IQR)	70.1 (28.1–125.3)	27.1 (8.4–75.5)	77.2 (35.8–133)	98.2 (30.5–168)						<0.001
Interleukin-6 in pg/mL, median (IQR)	39.8 (17.8–79.9)	20.2 (8.7–59)	44.3 (20.1–80.7)	65.8 (29.9–157.8)						<0.001
Ferritin in ng/mL, median (IQR)	676 (324.5–1135.8)	509 (202–1039)	706 (345–1207)	837 (334.3–1375)						0.051
Cardiovascular										
Heart rate per minute, median (IQR)	86 (75–98)	86 (75–99)	86 (75–98)	79.5 (70–90.8)						0.178
Systolic blood pressure in mmHg, median (IQR)	130 (119–140)	125 (118–135)	130 (120–145)	120 (109.3–139.3)						<0.001
Diastolic blood pressure in mmHg, median (IQR)	75 (70–80)	77 (70–80)	75 (70–80)	65 (55.5–70)						<0.001

<i>Respiratory tract</i>						
Dyspnea	498 (50.2)	69 (38.1)	399 (52.7)	30 (55.6)	0.002	
Cough	376 (37.9)	65 (35.9)	299 (39.5)	12 (22.2)	0.018	
Expectoration	31 (3.1)	2 (1.1)	27 (3.6)	2 (3.7)	0.247	
Respiratory rate per minute, median (IQR)	20 (16–26)	18 (16–24)	20 (16–26)	20 (16–30)	0.001	
Oxygen saturation (room air, pulse oximetry), median (IQR)	95 (92–97)	97 (96–98)	94 (91–96)	94 (89.3–96)	<0.001	
Arterial PaCO ₂ in mmHg, median (IQR)	5 (31.9–39)	35.3 (32–39)	35 (31.5–39)	34 (30–36.1)	0.002	
Lung infiltrates on chest radiography						
No infiltrate	342 (34.5)	133 (73.5)	188 (24.8)	21 (38.9)	<0.001	
Unilateral	244 (24.6)	33 (18.2)	198 (26.2)	13 (24.1)	0.053	
Bilateral	406 (40.9)	15 (8.3)	371 (49)	20 (37)	<0.001	
<i>Liver</i>						
Albumin in g/L, median (IQR)	28.7 (24.7–33.3)	31.8 (27.3–36.7)	28 (24.3–33)	25.9 (23.1–30.4)	<0.001	
Lactic acid dehydrogenase, in IU/L, median (IQR)	301 (229–400)	231 (187–313)	314 (243–406)	338 (241.3–486.5)	<0.001	
Bilirubin in mg/dl, median (IQR)	0.5 (0.36–0.68)	0.5 (0.38–0.68)	0.49 (0.4–0.7)	0.6 (0.4–0.9)	0.199	
<i>Renal/hydroelectrolytic</i>						
Creatinine in mg/dL, median (IQR)	0.9 (0.8–1.2)	0.9 (0.7–1.1)	0.9 (0.8–1.2)	3.2 (1.8–5.9)	<0.001	
Sodium in mEq/L, median (IQR)	137 (134–139)	138 (136–140)	136 (134–139)	136 (134–140)	<0.001	
Potassium in mEq/L, median (IQR)	3.8 (3.4–4.1)	3.9 (3.5–4.1)	3.7 (3.4–4)	4.4 (3.8–4.7)	<0.001	
<i>Hematological</i>						
Hemoglobin in g/L, median (IQR)	134 (118–146)	137 (118–153)	135 (120–146)	110 (97.3–122.8)	<0.001	
Hematocrit in %, median (IQR)	39.8 (35.7–43.4)	40.7 (35.2–45.1)	39.8 (36–43.3)	34.8 (30–37.8)	<0.001	
Platelet cells × 10 ³ /mm ³ , median (IQR)	190.5 (145–250)	194 (143–260)	188 (145–248)	212.5 (155.3–320.5)	0.362	
International normalized ratio, median (IQR)	1.2 (1.1–1.3)	1.15 (1.1–1.3)	1.2 (1.1–1.3)	1.3 (1.1–1.5)	0.003	
<i>Others</i>						
Creatine phosphokinase in IU/L, median (IQR)	98.5 (57–181)	86 (49–146)	102 (59–189)	81 (48.3–176.5)	0.007	
Blood glucose in mg/dL, median (IQR)	114 (98–139)	105 (92–126)	115 (100–140)	133.5 (105–200.8)	<0.001	

Values reported after multiple imputation (see study methods). AIDS: acquired immunodeficiency syndrome; COVID-19: coronavirus disease 2019; CI: confidence intervals; HIV: human immunodeficiency virus; IU: international units; IQR: interquartile range.

*Results are presented as No. of patients/total of patients unless otherwise indicated. Patients were assigned to the three phenotypes previously identified by Gutierrez-Gutierrez and colleagues following their probabilistic model (see study methods for more details) [4].

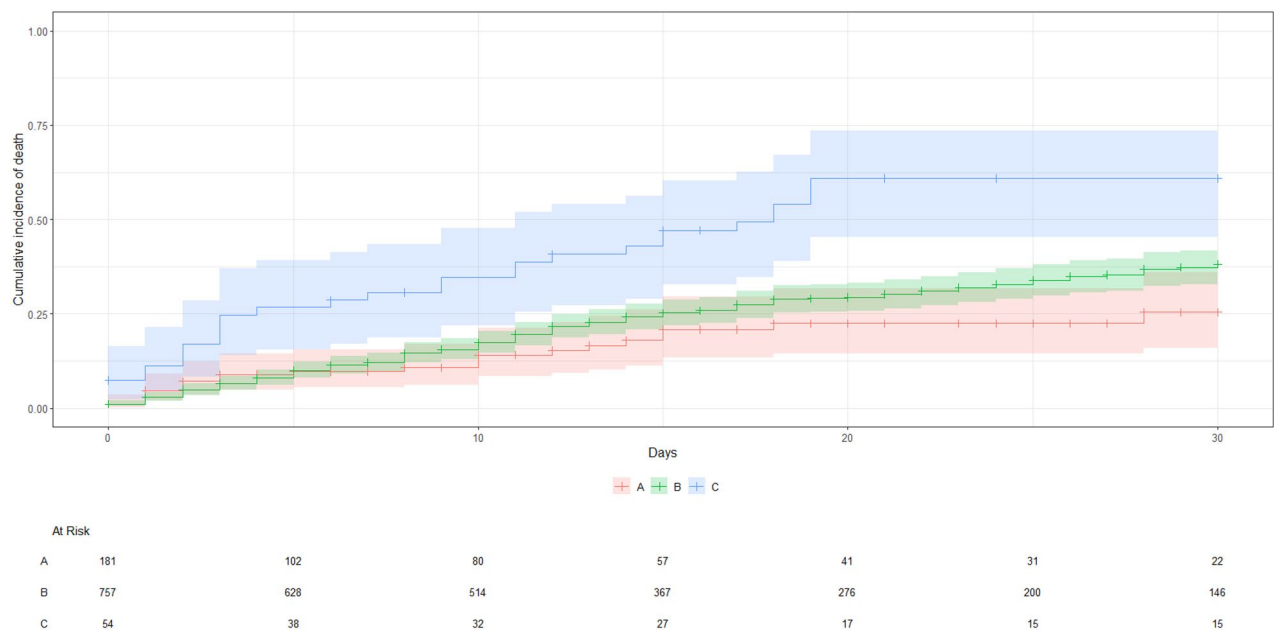


Figure 1. Cumulative mortality up to day 30 according to phenotypes developed by Gutierrez-Gutierrez and colleagues. Patients were assigned to the three phenotypes previously identified by Gutierrez-Gutierrez and colleagues following their probabilistic model (see study methods for more details) [4]. The time of origin is the day of hospital admission for COVID-19. Death is the event of interest and right-censoring was applied at the end of follow-up (hospital discharge or day 30, whichever came first).

for phenotype C vs. A (HR 3.10, 95% CI 1.81–5.30, $p < 0.001$) and for phenotype C vs. B (HR 2.20, 95% CI 1.50–3.23, $p < 0.001$). Although not statistically significant, an HR directed towards higher mortality was also observed for phenotype B vs. A (HR 1.41; 95% CI 0.92–2.15, $p = 0.115$).

With regard to secondary analyses, the demographic and clinical characteristics of patients were similar after the random assignment of patients to the derivation cohort or the internal validation cohort (supplementary Table S2). By means of cluster analysis, three phenotypes were identified in the derivation cohort (silhouette index 0.1). The identified phenotypes were named A1, B1, and C1. The letter of the phenotypes (A1, B1, and C1) was assigned based on the clinical similarity with the three phenotypes previously identified in the Spanish cohort. More in detail, we first noticed that the smallest phenotype in our cohort was similar to the smallest one in the Spanish cohort. Indeed, patients belonging to the smallest phenotype in our cohort, like patients belonging to phenotype C in the Spanish cohort, showed both an increased burden of baseline comorbidities and a more severe clinical presentation of COVID-19 (e.g. higher frequency of dyspnea, lower peripheral oxygen saturation) when compared with the entire derivation cohort. Therefore, we named the smallest phenotype in our cohort phenotype C1. Subsequently, we noticed that, unlike in the Spanish cohort, there was not a far larger phenotype in terms

of the number of patients among the remaining two phenotypes identified in our derivation cohort, and that the two phenotypes also presented a similar distribution of COVID-19-related signs and symptoms and of laboratory parameters. Nonetheless, as in the Spanish cohort, we noticed that patients belonging to one of the two remaining phenotypes had a very reduced burden of comorbidities compared with the entire derivation cohort. This phenotype was thus named phenotype A1 after the Spanish phenotype which also showed a considerably reduced burden of comorbidities (phenotype A). The last remaining phenotype was named phenotype B1. Of note, as many as 66% of patients assigned to the FEN-COVID-19 phenotype A in our cohort had a probability $< 70\%$ to be assigned to phenotype A. Thus, there was not a large difference between their probability to be assigned to phenotype A vs. phenotype B. In line with this similarity, while most of the patients in our cohort who were assigned to phenotype A by the FEN-COVID-19 model were also assigned to phenotype A1 in our derivation cohort (77/124, 62%), the majority of patients belonging to phenotype A1 in our derivation cohort were assigned to phenotype B by the FEN-COVID-19 model (225/314, 72%). The distribution of demographic and clinical variables in the three phenotypes A1, B1, and C1 is shown in Table 2 and presented graphically by means of a chord diagram and heatmap in Figure 2 and supplementary figure S1, respectively.

Table 2. Demographic and clinical characteristics of patients in the derivation cohort and in the phenotypes obtained by cluster analysis*.

Variable	Entire derivation cohort		Phenotype A1		Phenotype B1		Phenotype C1		P value
	No. of patients (%)	No. of patients (%)	No. of patients (%)	No. of patients (%)	No. of patients (%)	No. of patients (%)	No. of patients (%)		
Demographics									
Age in years, median (IQR)	72 (60-82)	67 (55-79)	75 (65.2-85)	72.5 (65.8-84)					<0.001
Male sex	408 (62)	193 (62)	175 (61)	40 (71)					0.329
Comorbidities									
Chronic heart disease	61 (9)	19 (6)	34 (12)	s8 (14)					0.002
Hypertension	317 (48)	112 (36)	172 (60)	33 (59)					<0.001
Chronic lung disease	74 (11)	0 (0)	60 (21)	14 (25)					<0.001
Chronic kidney disease	56 (9)	12 (4)	37 (13)	7 (13)					<0.001
Chronic liver disease	23 (4)	0 (0)	1 (0)	22 (39)					<0.001
Chronic neurological disease	91 (14)	0 (0)	84 (29)	7 (13)					<0.001
Active solid malignancy	39 (6)	0 (0)	33 (12)	6 (11)					<0.001
Active hematological malignancy	21(3)	0 (0)	18 (6)	3 (5)					<0.001
HIV/AIDS	10 (2)	3 (1)	3 (1)	4 (7)					0.002
Obesity	27 (4)	0 (0)	25 (9)	2 (4)					<0.001
Diabetes mellitus	106 (16)	37 (12)	44 (15)	25 (45)					<0.001
Dementia	65 (10)	13 (4)	45 (16)	7 (13)					<0.001
Treatments for underlying conditions									
Angiotensin converting enzyme inhibitors	94 (14)	0 (0)	85 (30)	9 (16)					<0.001
Angiotensin receptor blockers	95 (15)	48 (15)	42 (15)	5 (9)					0.457
Infection data at diagnosis									
Non-focal symptoms									
Reported fever	511 (78)	263 (84)	209 (73)	39 (70)					0.002
Temperature in °C, median (IQR)	37.1 (36-38)	37.2 (36.4-38)	37.1 (36-38)	37 (36-37.9)					0.623
Myalgia/arthralgia	31 (5)	0 (0)	31 (11)	0 (0)					<0.001
Headache	13 (2)	4 (1)	9 (3)	0 (0)					0.139
Anosmia	15 (2)	8 (3)	6 (2)	1 (2)					0.903
Altered mental status	66 (10)	16 (5)	42 (15)	8 (14)					<0.001
Inflammation									
White blood cells × 10 ³ /mm ³ , median (IQR)	6.7 (5-9.5)	6.7 (5-8.7)	6.4 (4.8-9.1)	10.3 (6.3-15.1)					<0.001
Lymphocyte cells × 10 ³ /mm ³ , median (IQR)	0.9 (0.6-1.2)	0.9 (0.6-1.2)	0.9 (0.6-1.2)	1.3 (0.6-2.2)					0.006
Neutrophil cells × 10 ³ /mm ³ , median (IQR)	6.7 (5-9.5)	6.7 (5-8.7)	6.4 (4.8-9.1)	10.3 (6.3-15.1)					0.001
D-dimer in ng/mL, median (IQR)	1004 (604-1782)	983.8 (595.4-1619)	1059(599.8-1842)	1017.5 (639.2-2250.5)					0.448
Procalcitonin in ng/mL, median (IQR)	0.2 (0.1-0.4)	0.2 (0.1-0.4)	0.2 (0.1-0.3)	0.3 (0.1-1.1)					0.040
C-reactive protein in mg/L, median (IQR)	71.6 (28.2-124.2)	74.7 (27.7-131)	71.2 (29.8-118.8)	64.2 (21.7-111.8)					0.660
Interleukin-6 in pg/mL, median (IQR)	39 (17.3-85.9)	37.7 (16.1-77.3)	41.6 (18.9-82.2)	58 (15.8-158.2)					0.259
Ferritin in ng/mL, median (IQR)	656 (285.8-1185.8)	649.5 (312.8-1204.2)	657 (282.5-1130)	753.5 (236-1187.8)					0.971
Cardiovascular									
Heart rate per minute, median (IQR)	86 (75-100)	87 (76-100)	85 (72-100)	85.5 (77.5-98)					0.104
Systolic blood pressure in mmHg, median (IQR)	130 (118-145)	130 (120-148.5)	130 (116.2-141.8)	125 (115-140)					0.050
Diastolic blood pressure in mmHg, median (IQR)	75 (70-80)	75 (70-82.8)	75 (68.5-80)	70 (60-80)					0.014
Respiratory tract									
Dyspnea	338 (52)	160 (51)	143 (50)	35 (63)					0.222
Cough	235 (36)	122 (39)	100 (35)	13 (23)					0.074
Expectoration	21 (3)	0 (0)	21 (7)	0 (0)					<0.001
Respiratory rate per minute, median (IQR)	20 (16-25)	20 (16-24)	20 (16-26)	22 (17.5-30)					0.091

Table 2. Continued.

Variable	Entire derivation cohort			Phenotype A1 No. of patients (%) 314 (48)	Phenotype B1 No. of patients (%) 286 (44)	Phenotype C1 No. of patients (%) 56 (8)	P value
	No. of patients (%) 656 (100)	No. of patients (%) 95 (91-97)	No. of patients (%) 35 (31-39)				
Oxygen saturation (room air, pulse oximetry), median (IQR)	95 (91-97)	95 (92-97)	35 (31-39)	94 (91-9)	91.5 (86-97)	0.002	
Arterial PaCO ₂ in mmHg, median (IQR)	35 (32-40)	35 (31-39)	35 (31-39)	36.2 (32-40)	36 (32-41)	0.036	
Lung infiltrates on chest radiography	215 (33)	102 (33)	87 (30)	87 (30)	26 (46)	0.065	
No. infiltrate	164 (25)	72 (23)	79 (28)	79 (28)	13 (23)	0.394	
Unilateral	277 (42)	140 (45)	140 (45)	120 (42)	17 (30)	0.138	
Bilateral							
<i>Liver</i>							
Albumin in g/L, median (IQR)	29.4 (25.2-34.5)	29.1 (25.2-34.5)	29.1 (25.2-34.5)	30.1 (25.3-24.5)	26.8 (24.5-33.5)	0.163	
Lactic acid dehydrogenase, in IU/L, median (IQR)	304 (225-395.5)	311.5 (238-404.5)	311.5 (238-404.5)	295.5 (214.5-381.5)	276.5 (212.2-368.8)	0.047	
Bilirubin in mg/dl, median (IQR)	0.5 (0.4-0.7)	0.5 (0.4-0.7)	0.5 (0.4-0.7)	0.5 (0.4-0.7)	0.5 (0.4-0.7)	0.552	
<i>Renal/hydroelectrolytic</i>							
Creatinine in mg/dL, median (IQR)	0.9 (0.8-1.2)	0.9 (0.8-1.1)	0.9 (0.8-1.1)	1 (0.8-1.3)	1 (0.8-1.2)	0.017	
Sodium in mEq/L, median (IQR)	137 (134-139)	137 (134-139)	137 (134-139)	136 (134-140)	137.5 (135-141)	0.218	
Potassium in mEq/L, median (IQR)	3.7 (3.4-4.1)	3.7 (3.4-4.1)	3.7 (3.4-4.1)	3.7 (3.4-4.1)	3.9 (3.6-4.2)	0.081	
<i>Hematological</i>							
Hemoglobin in g/L, median (IQR)	135 (119-147)	135 (119-147)	136 (124-148)	135 (117-146)	120.5 (106.2-140.5)	<0.001	
Hematocrit in %, median (IQR)	39.8 (35.7-43.5)	39.8 (35.7-43.5)	40.2 (36.6-43.6)	39.9 (35.4-43.5)	37.1 (32.9-42.3)	0.005	
Platelet cells × 10 ³ /mm ³ , median (IQR)	192 (147.8-254)	199 (155-264.8)	199 (155-264.8)	183 (139.239.8)	217.5 (153.8-319.5)	0.005	
International normalized ratio, median (IQR)	1.2 (1.1-1.3)	1.2 (1.1-1.3)	1.2 (1.1-1.3)	1.2 (1.1-1.3)	1.2 (1.1-1.4)	0.367	
<i>Others</i>							
Creatine phosphokinase in IU/L, median (IQR)	100 (57-180.5)	98 (61.2-174.8)	98 (61.2-174.8)	101.5 (56.2-221)	86.5 (39-164.5)	0.312	
Blood glucose in mg/dL, median (IQR)	113.5 (97-139.2)	111.5 (97.2-132)	111.5 (97.2-132)	115 (97-141)	128.5 (32-228.8)	0.016	

Values reported after multiple imputations (see study methods). AIDS, acquired immunodeficiency syndrome; COVID-19, coronavirus disease 2019; CI, confidence intervals; HIV, human immunodeficiency virus; IU, international units; IQR, interquartile range.

* Results are presented as No. of patients/total of patients unless otherwise indicated. Patients were assigned to the different phenotypes by cluster analysis (see study methods for more details).

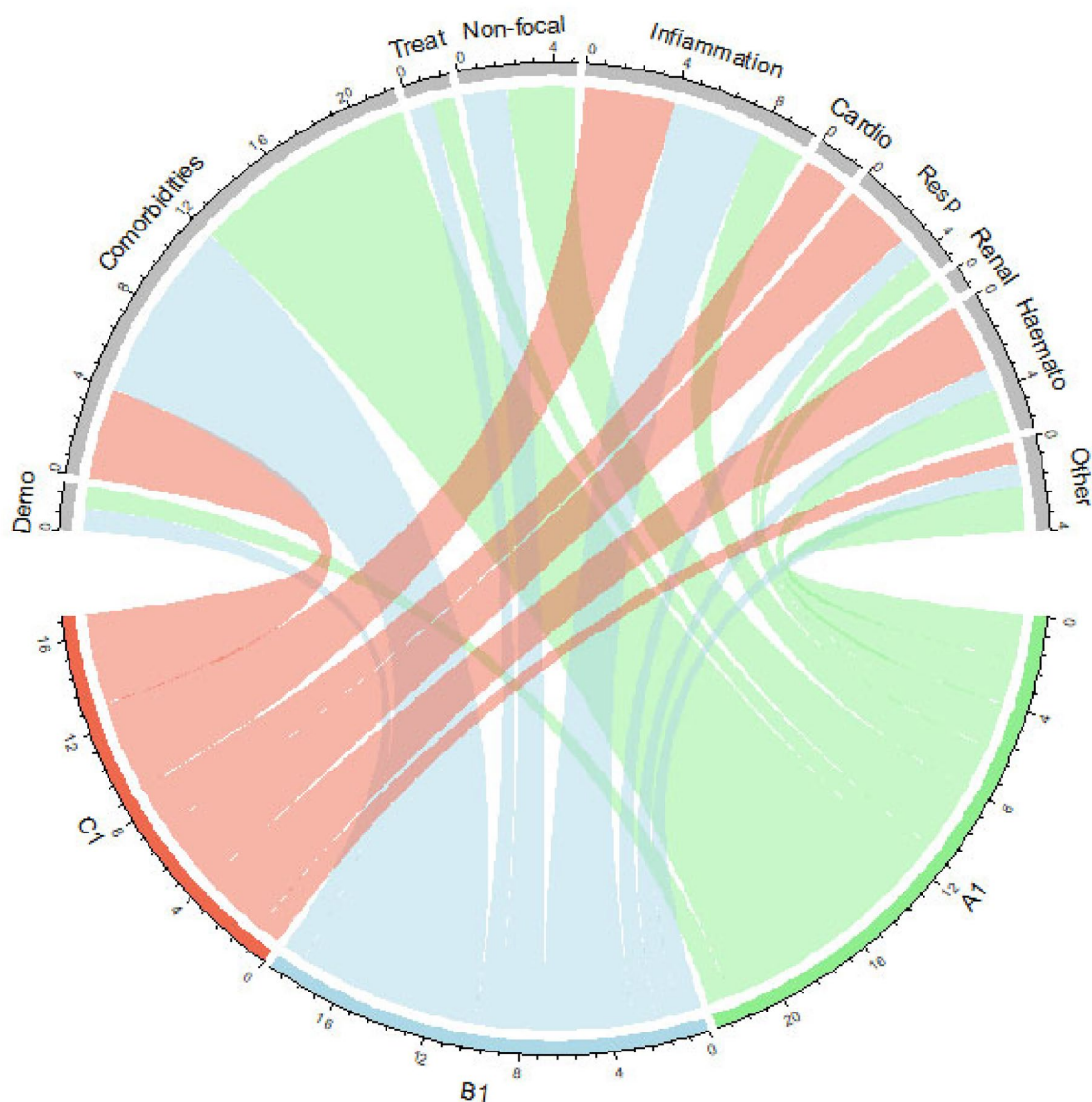


Figure 2. Chord diagram of the distribution of variable groups in the different phenotypes in the derivation cohort. The variables are grouped into categories (Demo stands for Demographics, Treat stands for Treatments, Cardio stands for Cardiovascular, Resp stands for Respiratory, Haemato stands for Haematological), with the different colors representing the different phenotypes: green for phenotype A, blue for phenotype B, and red for phenotype C. A ribbon is connecting phenotypes to the different variable groups if the proportion (in the case of categorical variables) or the mean (in the case of continuous variables) is significantly different when compared to the entire derivation cohort. The width of the ribbon depends on the number of significantly correlated variables.

The subsequent step was the development of a parsimonious probabilistic model for the assignment of patients to the three phenotypes identified in our derivation cohort, following the methods used by Gutierrez-Gutierrez and colleagues. The crude associations we found between variables and the different phenotypes are reported in [Supplementary table S3](#). Overall, 34 variables were included in the final multinomial regression model (age, lymphocyte cell count, procalcitonin, heart rate, systolic blood pressure, respiratory rate, oxygen saturation, arterial PaCO₂, albumin,

lactic acid dehydrogenase, creatinine, potassium, hematocrit, platelet count, blood glucose, chronic heart disease, hypertension, chronic lung disease, chronic kidney disease, chronic neurologic disease, active solid malignancy, active hematological malignancy, HIV/AIDS, obesity, diabetes mellitus, dementia, treatment with angiotensin-converting enzyme inhibitors, reported fever, myalgia/arthritis, headache, altered mental status, cough, expectoration, lung infiltrates on chest radiography), as detailed in [Supplementary Table S4](#). Based on the actual

belonging of patients to the different phenotypes in the derivation cohort, the AUROC of the model for phenotype assignment was 0.96 (95% CI 0.94–0.97), 0.95 (95% CI 0.94–0.97), and 0.77 (95% CI 0.71–0.84) for phenotype A1, phenotype B1, and phenotype C1, respectively. The cumulative 30-day mortality in the derivation cohort was 48.8% in patients belonging to phenotype C1, while it was 36.8% and 41.7% in patients belonging to phenotype A1 and phenotype B1, respectively (supplementary Figure S2). An association with mortality in Cox regression models was observed for phenotype C1 vs. A1 (HR 1.72, 95% CI 1.07–2.76, $p=0.025$). Although not statistically significant, an HR directed towards higher mortality was observed for phenotype C1 vs. B1 (HR 1.31, 95% CI 0.83–2.07, $p=0.252$), and for phenotype B1 vs. A1 (HR 1.32; 95% CI 0.96–1.81, $p=0.089$).

After having assigned, using the multinomial regression model, the patients of the internal validation cohort to the three phenotypes that were identified in the derivation cohort (Supplementary Table S5), the final step was to assess mortality according to the different phenotypes also in the internal validation cohort. The cumulative 30-day mortality in the internal validation cohort is shown in supplementary Figure S3. Although not statistically significant, an HR directed towards higher mortality was observed for phenotype C1 vs. A1 (HR 2.79, 95% CI 0.85–9.19, $p=0.09$) and for phenotype C1 vs. B1 (HR 1.22, 95% CI 0.38–3.92, $p=0.74$), whereas a statistically significant association with mortality was observed for phenotype B1 vs. A1 (HR 2.28; 95% CI 1.43–3.65, $p<0.001$). A summary of cumulative 30-day mortality in the different study cohorts according to the different phenotypes is available in supplementary Table S6.

Discussion

In this study, we externally confirmed the prognostic impact of phenotypes previously identified by Gutierrez-Gutierrez and colleagues in a Spanish cohort, and the usefulness of their simplified probabilistic model for phenotypes assignment, although we observed less difference in mortality between phenotype A and B than in the Spanish cohort [4].

As in the Spanish cohort, the highest mortality was observed in patients assigned to phenotype C, whereas the lowest was observed in patients assigned to phenotype A. As in the Spanish cohort, patients assigned to phenotype C by the probabilistic model showed laboratory results suggestive of a hyper inflammatory state, the highest frequency of dyspnea, and the lowest peripheral oxygen saturation at

hospital admission, whereas patients assigned to phenotype A were the youngest and showed the lowest burden of baseline comorbidities. Finally, as in the Spanish cohort, most patients were assigned to phenotype B, composed of patients with a heavier burden of comorbidities than patients assigned to phenotype A, but with a less severe COVID-19 clinical presentation than patients assigned to phenotype C [4]. As anticipated above, a worth noting difference is that, while mortality rates were overall similar to those observed in the Spanish cohort for both phenotype B and phenotype C, 30-day mortality for phenotype A was far higher in our cohort than in the Spanish cohort (25.5% vs. 2.5%). While part of this difference may be related to the fact that, due to the unavailability of subsequent follow-up, patients were right-censored at hospital discharge (this may have biased results towards higher mortality considering that, in reality, risk of death in discharged patients was likely reduced in most cases due to improved clinical conditions), it should also be noted that, differently from the Spanish cohort, patients assigned to phenotype A in our cohort had more marked alterations of laboratory parameters and of peripheral oxygen saturation at admission than those belonging to phenotype A in the Spanish cohort, despite a similar low burden of baseline comorbidities. Overall, this may reflect different hospitalization criteria, considering that, among patients with no significant baseline comorbidities, only those with impaired respiratory function and alterations of laboratory results consistent with moderate to severe disease were admitted to our hospital during the first waves of the pandemic [12]. Nonetheless, this also highlights an important limitation to be considered when using phenotypes in clinical practice, that is, mortality is not inherently very low if a patient is assigned to phenotype A by the model, since, based on the patient's characteristics, the probability to be assigned to phenotype B may be only slightly lower than that to be assigned to phenotype A, in turn influencing mortality.

Notably, the differences mentioned above between our cohort and the Spanish cohort regarding patients with phenotype A could also explain why we were only partly able to reproduce phenotype development in our cohort. Indeed, while the prognostic effect of the phenotypes developed in our cohort was eventually similar to those developed in the Spanish cohort (the direction of the effect in Cox regression models was constantly towards higher mortality for phenotype C1 vs. A1, C1 vs. B1, and B1 vs. A1 both in our derivation cohort and in our internal validation cohort), cluster analysis in the

derivation cohort did not identify a far larger phenotype B1 than A1 (in terms of a number of patients) as for B vs. A in the Spanish cohort. In our opinion, this could reflect an increased difficulty in distinguishing phenotypes B1 and A1 based on laboratory results and respiratory function parameters in comparison with the Spanish cohort. Eventually, we think all of this further strengthen our primary validation analysis of the prognostic impact of the phenotypes identified by Gutierrez–Gutierrez and colleagues, since we were able to reproduce their results despite some notable differences between the Italian cohort and the Spanish cohort. Of note, three different phenotypes were also identified by Luszczek and colleagues among 1000 hospitalized patients with COVID-19 in a retrospective study conducted in 14 US hospitals, using ensemble clustering [3]. The authors observed a distribution of variables and prognostic impact across the three different phenotypes that were overall similar to those observed in our cohort and in the Spanish cohort, but with a less striking difference in terms of baseline comorbidities between the two phenotypes associated with the lowest mortality rates. In our opinion, this third variation further supports the underlying existence of three universal phenotypes that conferred a different risk of death in hospitalized COVID-19 patients during the first waves of the pandemic, and that could be generalized despite the presence of some differences across cohorts [3].

Certainly, the small sample of patients belonging to phenotype C1 in our secondary analyses, especially in the internal validation cohort, is an important limitation that must be acknowledged. Indeed, this could have precluded a solid validation of phenotypes development as a secondary analysis. In addition, the small dimension of our internal validation cohort did not allow us to attempt phenotype development also in this cohort. With regard to our primary study analysis (validation of the prognostic impact of the phenotypes identified by Gutierrez–Gutierrez and colleagues), which was conducted in the entire study population, a limitation worth reporting is that the available data allowed us to retrospectively collect 75.4% (52/69) of the total features employed by Gutierrez–Gutierrez and colleagues for phenotypes development [12]. However, it is also worth noting that the 17 features not included in our analyses were not associated with phenotypes in the study by Gutierrez–Gutierrez and colleagues and eventually not included in their probabilistic phenotype assignment model; thus, they had no effect on our primary validation analysis.

In conclusion, the prognostic impact of phenotypes previously identified by Gutierrez–Gutierrez and colleagues was confirmed in our external Italian cohort, although with less difference in mortality between phenotypes A and B than in the original study. Keeping in mind this limitation, our results could indirectly support the validity of both phenotypes development and their extrapolation to other hospitals and countries for management decisions during other possible future viral pandemics.

Acknowledgments

We would like to thank all the patients and their families, and all healthcare professionals for their daily dedication to the care of patients, as well as the employees of University of Genoa and all private donors who generously contributed. We would also like to thank the GECOVID study group of IRCCS Ospedale Policlinico San Martino: Anna Alessandrini; Marco Camera; Emanuele Delfino; Andrea De Maria; Chiara Dentone; Antonio Di Biagio; Ferdinando Dodi; Antonio Ferrazin; Giovanni Mazzarello; Malgorzata Mikulska; Laura Nicolini; Federica Toscanini; Daniele Roberto Giacobbe; Antonio Vena; Lucia Taramasso; Elisa Balletto; Federica Portunato; Eva Schenone; Nirmala Rosseti; Federico Baldi; Marco Berruti; Federica Briano; Silvia Dettori; Laura Labate; Laura Magnasco; Michele Mirabella; Rachele Pincino; Chiara Russo; Giovanni Sarteschi; Chiara Sepulcri; Stefania Tutino (Clinica di Malattie Infettive); Roberto Pontremoli; Valentina Beccati; Salvatore Casciaro; Massimo Casu; Francesco Gavaudan; Maria Ghinatti; Elisa Gualco; Giovanna Leoncini; Paola Pitto; Kassem Salam (Clinica di Medicina interna 2); Angelo Gratarola; Mattia Bixio; Annalisa Amelia; Andrea Balestra; Paola Ballarino; Nicholas Bardi; Roberto Boccafogli; Francesca Caserza; Elisa Calzolari; Marta Castelli; Elisabetta Cenni; Paolo Cortese; Giuseppe Cuttone; Sara Feltrin; Stefano Giovinazzo; Patrizia Giuntini; Letizia Natale; Davide Orsi; Matteo Pastorino; Tommaso Perazzo; Fabio Pescetelli; Federico Schenone; Maria Grazia Serra; Marco Sottano (Anestesia e Rianimazione; Emergenza Covid padiglione 64); Iole Brunetti; Maurizio Loconte; Lorenzo Ball; Denise Battaglini; Chiara Robba; Nicolò Patroniti (Anestesiologia e Terapia Intensiva); Roberto Tallone; Massimo Amelotti; Marie Jeanne Majabò; Massimo Merlini; Federica Perazzo (Cure Intermedie); Nidal Ahamd; Paolo Barbera; Marta Bovio; Paola Campodonico; Andrea Collidà; Ombretta Cutuli; Agnese Lomeo; Francesca Fezza; Nicola Gentilucci; Nadia Hussein; Emanuele Malvezzi; Laura Massobrio; Giulia Motta; Laura Pastorino; Nicoletta Pollicardo; Stefano Sartini; Paola Vacca; Valentina Virga (Dipartimento di Emergenza ed Accettazione); Italo Porto; Gian Paolo Bezante; Roberta Della Bona; Giovanni La Malfa; Alberto Valbusa; Vered Gil Ad (Clinica Malattie Cardiovascolari); Emanuela Barisione; Michele Bellotti; Aloe' Teresita; Alessandro Blanco; Marco Grosso; Maria Grazia Piroddi (Pneumologia ad Indirizzo Interventistico); Paolo Moscatelli; Paola Ballarino; Matteo Caiti; Elisabetta Cenni; Patrizia Giuntini; Ottavia Magnani (Medicine d'Urgenza); Samir Sukkar; Ludovica Cogorno; Raffaella Gradasci; Erica Guiddo; Eleonora Martino; Livia Pisciotta (Dietetica e Nutrizione clinica); Bruno

Cavagliere; Rossi Cristina; Farina Francesca (Direzione delle Professioni Sanitarie); Giacomo Garibotto; Pasquale Esposito (Clinica nefrologica, Dialisi e Trapianto); Giovanni Passalacqua; Diego Bagnasco; Fulvio Braido; Annamaria Riccio; Elena Tagliabue (Clinica Malattie Respiratorie ed Allergologia); Claudio Gustavino; Antonella Ferraiolo (Ostetricia e Ginecologia); Salvatore Giuffrida; Nicola Rosso (Direzione Amministrativa); Alessandra Morando; Riccardo Papalia; Donata Passerini; Gabriella Tiberio (Direzione di Presidio); Giovanni Orengo; Alberto Battaglini (Gestione del Rischio Clinico); Silvano Ruffoni; Sergio Caglieris.

Data availability statement

The data that support the findings of this study are available from the corresponding author upon reasonable request.

Author contributions

Conceptualization: D.R.G.; methodology: D.R.G., A.S., C.M., E.D.M., A.S.T., G.I., and M.Bas.; formal analysis and investigation: D.R.G., A.S., C.M., S.M., M.G., M.P.S., and G.D.M.; data collection, M.Bav., M.M., B.Bi., B.Br., G.C., C.S.T., A.V., A.D.B., C.D., C.R., L.B., A.O., I.B., P.P., D.B., and S.M.; writing—original draft preparation, D.R.G., A.S., and C.M.; writing—review and editing, D.R.G., E.D.M., A.S.T., M.Bav., C.S.T., C.M., G.D.M., G.C., B.Bi., S.M., A.S., A.V., M.M., C.D., B.Br., A.O., C.R., L.B., I.B., D.B., A.D.B., M.P.S., P.P., M.G., G.I., and M.Bas.; supervision: D.R.G., E.D.M., A.S.T., G.I., and M.Bas. All authors have read and approved the published version of the manuscript. All authors agree to be accountable for all aspects of the work.

Disclosure statement

Daniele Roberto Giacobbe is a section editor of *Annals of Medicine*. He had no role in the editorial process and decisions regarding the present article. Outside the submitted work, Daniele Roberto Giacobbe reports investigator-initiated grants from Pfizer, Shionogi, and Gilead Italia, and speaker/advisor fees from Pfizer and Tillotts Pharma. Outside the submitted work, Matteo Bassetti has received funding for scientific advisory boards, travel, and speaker honoraria from Angelini, Astellas, BioMérieux, Cidara, Gilead, Menarini, MSD, Pfizer, Shionogi, Tetrphase, Nabriva. The other authors have no conflicts of interests to disclose.

Funding

The present work was partly supported by “donazioni per ricerca scientifica su coronavirus” to the Department of Health Sciences (DISSAL), University of Genoa, and by “fondi donazioni COVID-19” to IRCCS Ospedale Policlinico San Martino.

ORCID

Emilio Di Maria  <http://orcid.org/0000-0002-8357-2658>
 Bianca Bruzzone  <http://orcid.org/0000-0002-3456-1899>
 Chiara Robba  <http://orcid.org/0000-0003-1628-3845>
 Antonio Di Biagio  <http://orcid.org/0000-0003-1436-5089>
 Paolo Pelosi  <http://orcid.org/0000-0002-8459-2730>
 Daniele Roberto Giacobbe  <http://orcid.org/0000-0003-2385-1759>

References

- [1] Robba C, Battaglini D, Ball L, et al. Distinct phenotypes require distinct respiratory management strategies in severe COVID-19. *Respir Physiol Neurobiol*. 2020;279:1. Aug
- [2] Rello J, Storti E, Belliato M, et al. Clinical phenotypes of SARS-CoV-2: implications for clinicians and researchers. *Eur Respir J*. 2020 May;55(5): 2001028.
- [3] Luszczek ER, Ingraham NE, Karam BS, et al. Characterizing COVID-19 clinical phenotypes and associated comorbidities and complication profiles. *PLOS One*. 2021;16(3):e0248956.
- [4] Gutierrez-Gutierrez B, Toro D, Borobia MD, et al. Identification and validation of clinical phenotypes with prognostic implications in patients admitted to hospital with COVID-19: a multicentre cohort study. *Lancet Infect Dis*. 2021;21(6):783–12.
- [5] Teng C, Thampy U, Bae JY, et al. Identification of phenotypes among COVID-19 patients in the United States using latent class analysis. *Infect Drug Resist*. 2021;14:3865–3871.
- [6] Ozonoff A, Schaenman J, Jayavelu ND, et al. Phenotypes of disease severity in a cohort of hospitalized COVID-19 patients: results from the IMPACC study. *EBioMedicine*. 2022;83:104208.
- [7] Lascarrou JB, Gaultier A, Soumagne T, et al. Identifying clinical phenotypes in moderate to severe acute respiratory distress syndrome related to COVID-19: the COVADIS study. *Front Med*. 2021;8:632933.
- [8] Tregoning JS, Flight KE, Higham SL, et al. Progress of the COVID-19 vaccine effort: viruses, vaccines and variants versus efficacy, effectiveness and escape. *Nat Rev Immunol*. 2021;21(10):626–636. Oct
- [9] Lin DY, Gu Y, Wheeler B, et al. Effectiveness of covid-19 vaccines over a 9-month period in North Carolina. *N Engl J Med*. 2022;386(10):933–941.
- [10] Heymans MW, Twisk JWR. Handling missing data in clinical research. *J Clin Epidemiol*. 2022;151:185–188.
- [11] Kosmidis I, Firth D. Multinomial logit bias reduction via the Poisson log-linear model. *Biometrika*. 2011;98(3):755–759.
- [12] Vena A, Giacobbe DR, Biagio D, et al. Clinical characteristics, management and in-hospital mortality of patients with coronavirus disease 2019 in Genoa, Italy. *Clin Microbiol Infect*. 2020;26(11):1537–1544. 2020 Nov